Journal of Electroceramics (2023) 50:44–49
https://doi.org/10.1007/s10832-023-00303-3

Effects of ZBS addition on crystallization, microstructure and dielectric properties of low temperature co-fired Mg_2SiO_4-$CaTiO_3$ ceramics

Cong Tang[1] · Yu Xin[1] · Caixia Zhang[2] · Jingang Tan[2] · Zugao Yu[2] · Chunchun Wu[3] · Jianxi Tong[2] · Fancheng Meng[1]

Received: 20 October 2022 / Accepted: 4 January 2023 / Published online: 19 January 2023

Abstract

The $0.9Mg_2SiO_4$-$0.1CaTiO_3$ (MSCT) ceramics with $60ZnO$-$20B_2O_3$-$20SiO_2$ glass (ZBS) and LiF compound additives were prepared by solid-state reaction method. The effects of different ZBS contents on the phase, densification temperature, surface morphology and dielectric properties of MSCT ceramics were studied. The results show that ZBS can inhibit the reaction between LiF and $CaTiO_3$, which improve the surface morphology and reduce the sintering temperature of MSCT ceramics. The sample of MSCT with 2wt%ZBS-1.5wt%LiF sintered at 900 °C for 90 min shows excellent microwave dielectric properties: $\varepsilon_r = 9.26$, $Q \times f = 68{,}580$ GHz (at 15.5 GHz) and $\tau_f = -1.49$ ppm/ °C. There is no obvious element diffusion at the co-firing interface between dielectrics and Ag electrodes, indicating it is a promising candidate for LTCC applications.

Keywords Low sintering temperature · High $Q \times f$ value · Near-zero τ_f · Microstructure

1 Introduction

With the rapid development of the fifth generation mobile communication technology (5G), the application of Massive MIMO and AAU RF technology puts forward higher requirements for the miniaturization, lightweight, integration and high frequency characteristics of components. Based on low temperature co-fired ceramics (LTCC), multilayer components with good high frequency performance, high integration and high reliability have a broad market prospect in 5G communication and future high frequency communication era [1–4].

LTCC materials should be sintered at around 900 °C or lower for co-firing with low melting point and highly conductive Ag electrodes [5, 6]. Forsterite (Mg_2SiO_4) ceramics, a candidate for millimeter-wave dielectrics materials, have low relative permittivity (ε_r) of 6.8 and high $Q \times f$ value of 270,000 GHz [7–11]. However, it has high sintering temperature (~1450 °C) and negative τ_f (-67 ppm/ °C), which limited its practical applications in LTCC field. Adding low melting point glass and oxide is a low cost and effective method to reduce the densification temperature of ceramics. Dou et al reported that $0.91Mg_2SiO_4$-$0.09CaTiO_3$ with 12wt% B_2O_3-Li_2O-SiO_2 glass was sintered at 950 °C, but the addition of glass greatly destroyed its $Q \times f$ value ($Q \times f$ ~ 11,300 GHz)a [11]. LiF have been proved to be suitable for reducing the densification temperature of Mg_2SiO_4 [11–14]. Ma et al reported that the Mg_2SiO_4-$0.24TiO_2$ with 4wt%LiF has shown $Q \times f$ of 31,091 GHz and a dielectric constant of 7.1 at a low sintering temperature of 950 °C [12]. However, the addition of LiF affects the surface morphology of Mg_2SiO_4, Zhang et al. [15] found that the addition of LiF led to the formation of abnormally grown grains and angular grains on the surface. In addition, the matching of Mg_2SiO_4 system with Ag paste has not been reported.

It is reported that ZnO-B_2O_3-SiO_2 glass (ZBS) is an effective low temperature sintering aid, and is used as a dopant to improve the sintering temperature of other material systems [16–18]. In this paper, LiF and ZBS were used as composite sintering aids, and $CaTiO_3$ was used as τ_f compensator. The effects of LiF-ZBS addition on the densification, crystalline phase, microstructure and microwave dielectric properties of $0.9Mg_2SiO_4$-$0.1CaTiO_3$ (MSCT) ceramics were

✉ Jianxi Tong
tongjianxi@bdstar.com

✉ Fancheng Meng
mengfancheng@cqut.edu.cn

[1] Department of Materials, Chongqing University of Technology, Chongqing 400054, China

[2] Jiaxing Glead Electronics Co. LTD, Jiaxing 314000, China

[3] Zhejiang-California International Nanosystems Institute, Zhejiang University, Hangzhou 310027, China

investigated. In addition, we also prepared the green tape by tape casting technology, and printed the Ag pattern by screen printing. The matching co-firing behavior of Ag electrode and ceramic green tape was studied.

2 Experimental procedure

The starting materials were MgO (≥99%, Duodian chemical, China), $CaCO_3$ (≥99%, Tongya chemical, China), SiO_2(≥99%, Fengcheng Reagent, Shanghai, China), TiO_2 (≥99.8%, Zhongxing, Xiantao, China), LiF, 60ZnO-20B_2O_3-20SiO_2 glass. Mg_2SiO_4 was weighed according to non-stoichiometric ratio of MgO:SiO_2=2.05:1 [19]. $CaTiO_3$ was weighed according to the chemical formulas. The powders were mixed with ethylalcohol and zirconia balls in a polyethylene bottle for 17 h, and then dried. The mixed $CaCO_3$-TiO_2 and powders MgO-SiO_2 were calcined at 1200 °C and 1250 °C for 3 h. Then, 0.9Mg2SiO_4-0.1$CaTiO_3$ powder mixed with 1.5wt % LiF + *x*wt % ZBS ($x = 0, 1, 2, 3, 4$) to reduces the sintering temperature. Mixture continues mixed with ethylalcohol and zirconia balls for 17h. Then the powders with 6wt%PVB pressed into green columns (6mm×4mm) at 180 MPa. Finally, These pellets were sintered at 840-930 °C for 90min in air.

The phase structures of the 0.9Mg_2SiO_4-0.1$CaTiO_3$ ceramics with 1.5wt% LiF- *x*wt% ZBS (*x*=0~4) sintered samples were confirmed using XRD radiation (Aeris, PANalytical, Holland) with Cu Ka. The bulk density of the sample was measured by Archimedes method. The microstructure of the sintered sample was examined using a scanning electron microscope (SEM, Phenom Pro X, Netherlands) and its composition was determined using an energy dispersive X-ray spectrometer (EDS). The relative permittivity (ε_r) and $Q \times f$ value of the samples was measured using a cavity and a network analyzer (10 MHz-43.5 GHz, KEY-SIGHT, N5232A). Placed the test cavity in a thermostat, and the frequency change in the temperature range of 25 °C -85 °C was recorded, the temperature coefficient of resonant frequency (τ_f) was calculated by the following formula:

$$\tau_f = \frac{f_{85\,^\circ C} - f_{25^\circ C}}{f_{25\,^\circ C}(85\ ^\circ\text{C} - 25\ ^\circ\text{C})} \quad (1)$$

3 Results and discussion

Fig. 1 shows the XRD patterns of MSCT ceramics with 1.5wt%LiF+ *x*ZBS ($x = 1$~4) ceramics sintered at their optimum sintering temperatures. According to the XRD pattern, the main crystalline phase of all the samples were Mg_2SiO_4 (ICDD no. #84-1402) and $CaTiO_3$ (ICDD no. #77-0182). The change of the second phase of the sample is closely related to the content of ZBS. LiF, CaF_2 and Li_2TiO_3 phase was detected when *x*=0. With the increase of *x*, the diffraction peaks of CaF_2 and Li_2TiO_3 decrease gradually and disappear when $x > 1$. SiO_2 was detected with an addition of *x*= 4. A possible mechanism is that $CaTiO_3$ reacts with LiF to form CaF_2 and Li_2TiO_3 for *x*=0. When $x > 0$, the addition of ZBS hindered the reaction between $CaTiO_3$ and LiF, and LiF promoted the crystallization of ZBS.

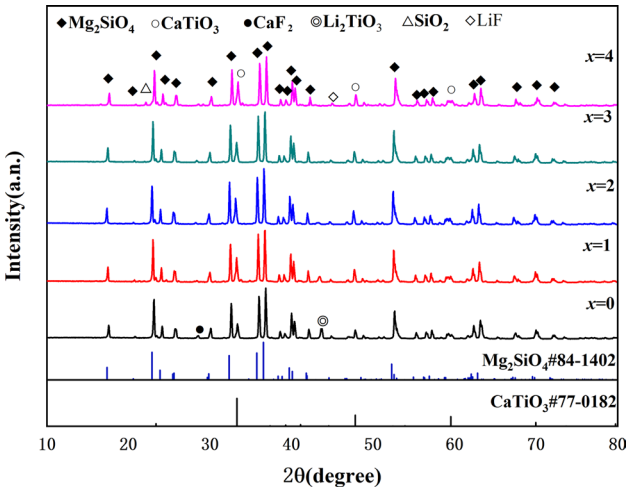

Fig. 1 XRD patterns of 0.9Mg_2SiO_4-0.1$CaTiO_3$ ceramics with 1.5wt% LiF-*x*wt% ZBS ($x = 0$~4) ceramics sintered at their optimum sintering temperatures

$$CaTiO_3 + 2LiF \rightarrow CaF_2 + Li_2TiO_3$$

Figure 2 shows the bulk density of (0.9Mg_2SiO_4-0.1$CaTiO_3$)-1.5wt%LiF-*x*wt%ZBS(*x*=0~4) ceramics sintered at different temperature. The results show that the bulk density of the sample is related to the sintering temperature

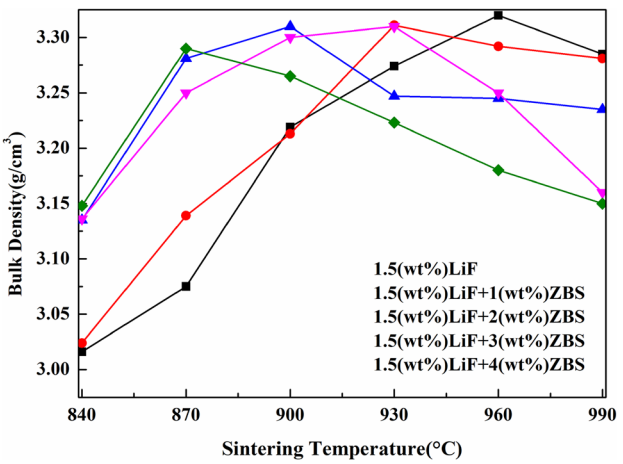

Fig. 2 The bulk density of (0.9Mg_2SiO_4-0.1$CaTiO_3$) -1.5wt%LiF-*x*wt%ZBS(*x*=0~4) ceramics sintered at different temperature

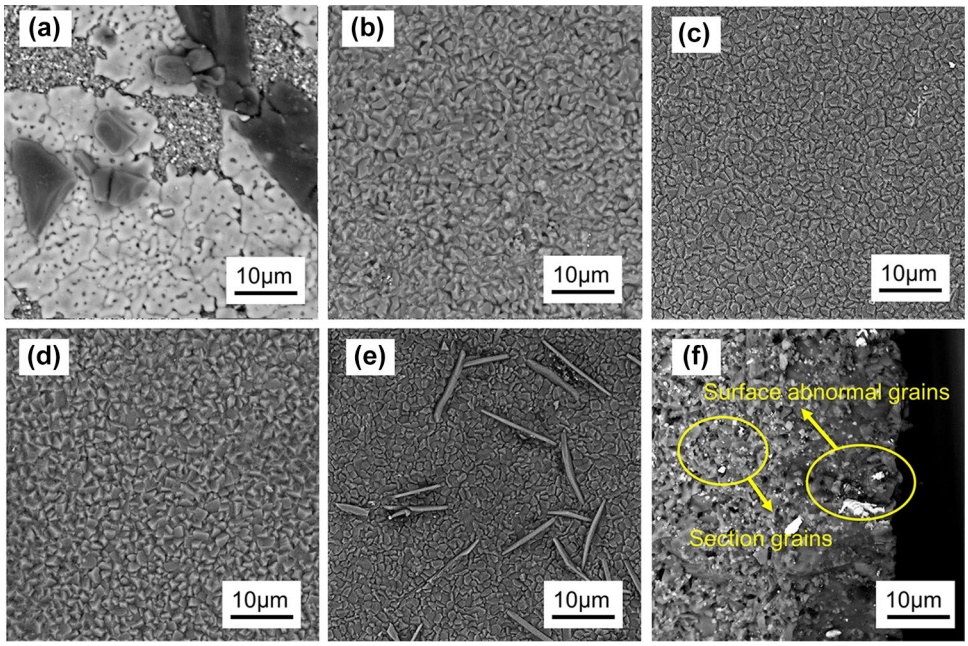

Fig. 3 SEM micrographs of ($0.9Mg_2SiO_4$-$0.1CaTiO_3$) +1.5wt%LiF+xZBS(x =0~4) ceramics sintered at their optimum sintering temperatures for different x values: (**a**) the surface of $x = 0$; (**b**) the surface of $x = 1$; (**c**) the surface of $x = 2$; (**d**) the surface of $x = 3$; (**e**) the surface of $x = 4$; (**f**) the section of x=0

and ZBS content. With the increase of sintering temperature, the density of the sample increases gradually due to the decrease of porosity and the growth of grains. When the sintering temperature reaches the densification temperature of the sample, the density begins to decrease due to overburning. In addition, with the increase of ZBS content, the densification temperature of the sample decreases [12, 13]. The density of the samples with 0, 1, 2,3,4wt % ZBS reached the maximum at 960 °C, 930 °C, 900 °C, 900 °C and 870 °C. The results show that with the increase of ZBS content, the densification mechanism of (0.9 Mg_2SiO_4-$0.1CaTiO_3$)-1.5wt%LiF-$x$wt%ZBS(x=0~4) samples moves to a lower temperature.

Figure 3 shows the SEM micrographs of the surface of ($0.9Mg_2SiO_4$-$0.1CaTiO_3$) +1.5wt%LiF+x ZBS (x =0~4) ceramics sintered at their optimum sintering temperatures for different x values. As shown, when $x = 0$, there are abnormally grown white and black grains on the surface. As shown in Figure 3(f), this situation only exists on the sample surface. Zhang et al. [15] reported a similar phenomenon in the study of the effect of LiF on the properties of Mg_2SiO_4, but did not explain it well. In order to further study the formation of surface abnormal grains, EDS was used to analyze the elemental composition of the grains, as shown in Fig. 4A and B was used to mark grains of different colors. The results show that the main elements of A was F and O, and the main elements of B was F, Ca, Mg, Si and O. It seems impossible to detect lithium using an EDS detector [20]. According to XRD analysis, when $x = 0$, the sample consists of Mg_2SiO_4 (ICDD no. #84-1402), $CaTiO_3$ (ICDD

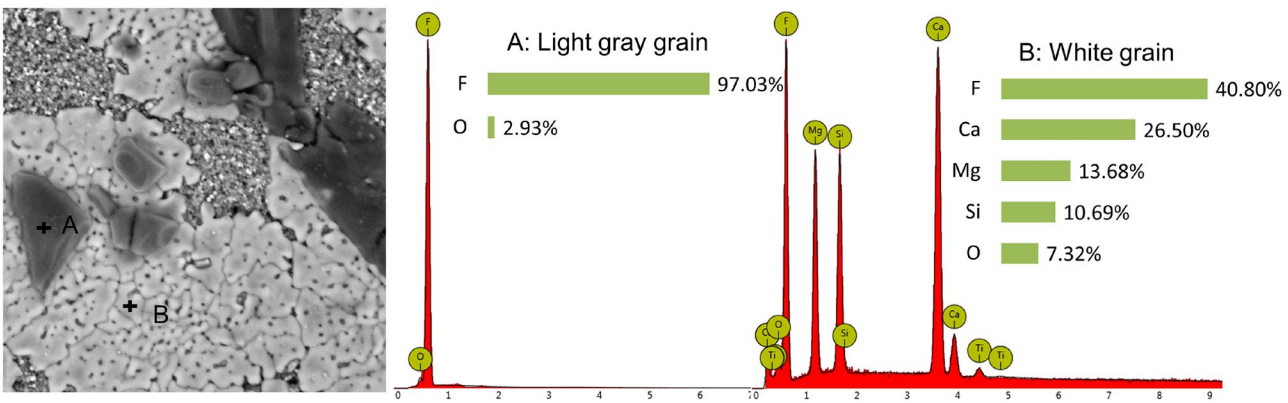

Fig. 4 The EDS datum of ($0.9Mg_2SiO_4$-$0.1CaTiO_3$) +1.5wt%LiFceramics sintered at 960 °C

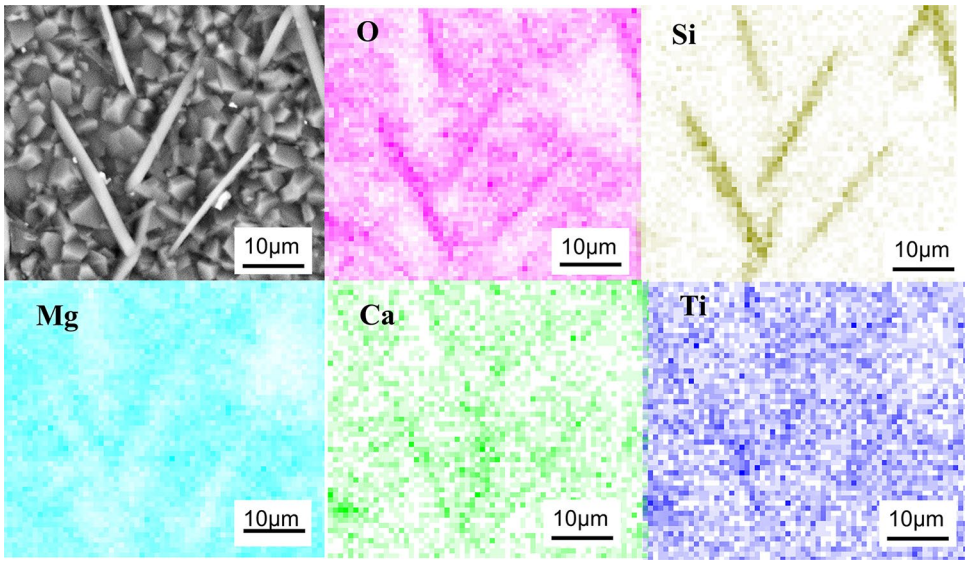

Fig. 5 The EDS datum of $(0.9Mg_2SiO_4\text{-}0.1CaTiO_3)$ +1.5wt%LiF+x ZBS ($x = 4$) ceramics sintered at 870 °C

no. #89-6949), and the second phases CaF, Li_2TiO_3 and LiF. respectively. It indicates that they are CaF_2 and LiF. With the addition of ZBS, the abnormal growth grains disappear and the sintering gradually becomes dense. When the content of ZBS exceeds 4wt %, the surface appears needle-like grains. As shown in Fig. 5, EDS shows that the Si content in the needle-like grains is higher. Eoh et al. [21] report that the presence of silicon-rich liquid phase led to abnormal growth of table-second grains in the study of $Zn_{1.8}SiO_4$. According to XRD analysis, when $x = 4$, the second phase SiO_2 appears. One possible reason is that LiF enters the ZBS glass network, interrupting the ZBS glass B-Si network, and LiF is absorbed. ZBS added crystallization. The results show that LiF is easy to diffuse to the surface of the sample and reacts with $CaTiO_3$ to form CaF_2 on the surface of the sample. LiF and CaF_2 grow abnormally on the surface. The addition of ZBS can prevent the diffusion of LiF to the surface, but too much ZBS can crystallize on the surface to form abnormally grown acicular grains.

Figure 6 shows the dielectric ε_r and $Q \times f$ values of $(0.9Mg_2SiO_4\text{-}0.1CaTiO_3)$ +1.5wt%LiF+x ZBS ($x = 0 \sim 4$) sintered at different temperature. It can be seen that with the increase of temperature and ZBS content, the dielectric constant ε_r and density show a similar trend, because the densification of ceramics has an important influence on the dielectric constant ε_r [20]. Figure 6(b) shows that the $Q \times f$ value increases first and then decreases with the increase of ZBS content and sintering temperature. When $x = 2$, the $Q \times f$ value of the ceramic sample reaches the maximum at 900 °C. As shown in Figure 3, with the increase of x, the grain becomes more and more dense, and $Q \times f$ is expected to increase. When x further increases, the $Q \times f$

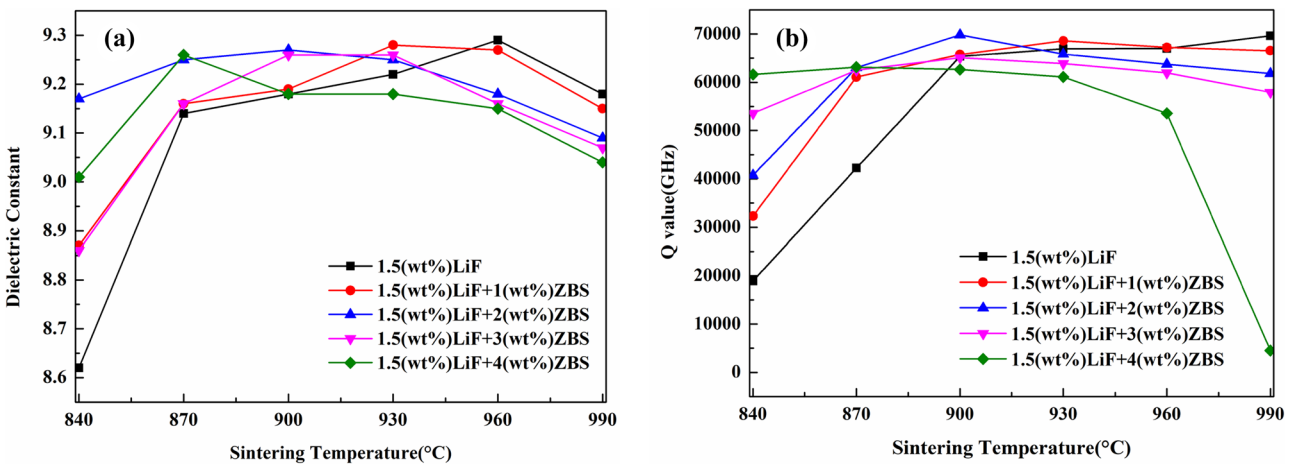

Fig. 6 The dielectric ε_r and $Q \times f$ values of $(0.9Mg_2SiO_4\text{-}0.1CaTiO_3)$ +1.5wt%LiF+x ZBS (x = 0~ 4) sintered at different temperature

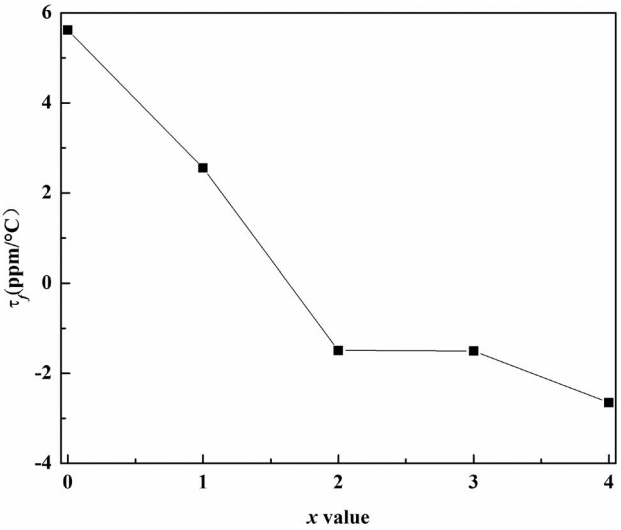

Fig. 7 The τ_f value of $(0.9Mg_2SiO_4\text{-}0.1CaTiO_3)$ +1.5wt%LiF+x ZBS ($x = 0 \sim 4$) at their optimum sintering temperatures

value decreases, which may be related to the abnormal grain growth.

Figure 7 shows the τ_f value of $(0.9Mg_2SiO_4\text{-}0.1CaTiO_3)$ +1.5wt%LiF+x ZBS ($x = 0 \sim 4$) at their optimum sintering temperatures. In general, τ_f is dependent on the structure, composition, the additive or the second phase of the materials. The composite value follows the mixing rule and the value is determined using For-mula [22].

$$\tau_f = V_1\tau_{f1} + V_2\tau_{f2} + V_3\tau_{f3}. \quad (2)$$

$$V_1 + V_2 + V_3 = 1.$$

Where τ_{f1} , τ_{f2} and τ_{f3} are the τ_f values of Mg_2SiO_4, $CaTiO_3$ and ZBS phases, respectively. The τ_f decreased slightly with an increase of ZBS(τ_f=-23ppm/ °C) content, changing from +5.62 ppm/ °C to -2.65 ppm/ °C. When the concentration of ZBS is 2wt %, the τ_f of $(0.9Mg_2SiO_4\text{-}0.1CaTiO_3)$ +1.5wt%LiF+2wt%ZBS composites is near to zero (τ_f=-1.49ppm/ °C).

In the LTCC production process, it is necessary to study the matching co-firing of Ag paste and ceramic green tape. In order to evaluate the chemical compatibility of $(0.9Mg_2SiO_4\text{-}0.1CaTiO_3)$ +1.5wt%LiF+$x$wt%ZBS (x=2) ceramics and electrode materials, the Ag paste was printed on the x = 2wt % ceramic green tape, and the EDS analysis and XRD spectrum of the Ag electrode co-firing sample at 900 °C were shown in Fig. 8. Figure 8(a) shows the surface line scan EDS image of the composite substrate. After sintering at 900 °C, the printed pattern is complete without diffusion. Through line scanning EDS analysis, it was found that Ag diffused in the joint surface and the Ag content changed dramatically. However, the content of Ag in the composites is close to zero. Figure 8(c) is the XRD spectrum of the composite substrate and porcelain belt. It can be seen from Fig. 8(c) that the phase before sintering is consistent with the subsequent sintering. No silver compound phase can be observed other than metallic silver (Ag, ICDD # 87-0597) compared to non-silver ceramics. The results show that there is no reaction between $(0.9Mg_2SiO_4\text{-}0.1CaTiO_3)$ +1.5wt%LiF+$x$wt%ZBS (x=2) ceramics and Ag electrode. Therefore, $(0.9Mg_2SiO_4\text{-}0.1CaTiO_3)$ +1.5wt%LiF+x ZBS (x = 2) ceramics with Ag chemical compatibility are promising LTCC materials.

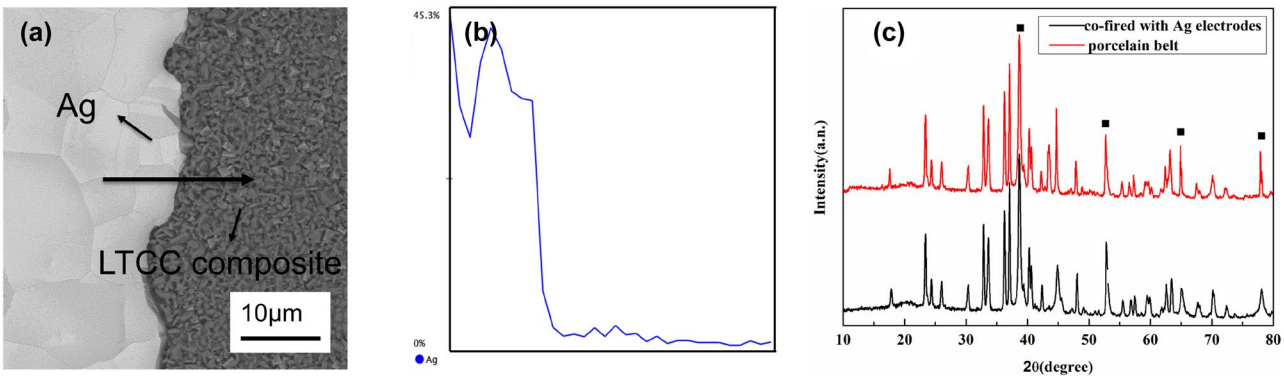

Fig. 8 SEM photograph of $(0.9Mg_2SiO_4\text{-}0.1CaTiO_3)$ +1.5wt%LiF+x ZBS (x = 2) samples co-fired with Ag sintering at 900 °C: (**a**) Surface image; (**b**) Line scanning EDS analysis of Ag diffusion profile; (**c**) XRD patterns of composites co-fired with Ag electrodes and porcelain belt

4 Conclusions

In this work, 1.5wt % Li F + *x*wt % ZBS additive was used as sintering additive, and the temperature coefficient of resonant frequency (τ_f) of Mg_2SiO_4 was adjusted by doping with $CaTiO_3$, which effectively reduced the sintering temperature of the material and improved its τ_f. The effects of different ZBS contents on the phase, densification temperature, surface morphology and dielectric properties of $0.9Mg_2SiO_4$-$0.1CaTiO_3$-1.5wt%LiF samples were studied. The results show that the addition of ZBS can inhibit the reaction between LiF and $CaTiO_3$, improve the surface morphology and reduce the sintering temperature. Therefore, when $x = 2$, the sintering temperature of the ceramics is effectively reduced from above 1450 °C to 900 °C, and the temperature coefficient of resonant frequency (τ_f) is modified to -1.49 ppm / °C, with high $Q \times f$ (68,583 GHz). In addition, ($0.9Mg_2SiO_4$-$0.1CaTiO_3$) + 1.5wt%LiF +2wt%ZBS ($x = 2$) LiF ceramics with Ag chemical compatibility are promising LTCC materials.

Acknowledgements This work was Supported by the "Pioneer" R&D Program of Zhejiang Province under 2022C01006.

Author contribution Jianxi Tong: Conceptualization, Methodology, Software. Cong Tang: Data curation, Writing- Original draft preparation. Yu Xin: Visualization, Investigation. Zugao Yu, Chunchun Wu: Supervision. Caixia Zhang, Jingang Tan: Software, Validation. Fancheng Meng:Writing- Reviewing and Editing.

Research data policy and data availability statements The data that support the findings of this study are available from the corresponding author upon resonable request.

Declarations

Conflict of interest No conflict of interest exits in the submission of this manuscript, and manuscript is approved by all authors for publication. I would like to declare on behalf of my co-authors that the work described was original research that has not been published previously, and not under consideration for publication elsewhere, in whole or in part. All the authors listed have approved the manuscript that is enclosed.

References

1. T.Y. Qin, C.W. Zhong, B. Tang et al., A novel type of composite LTCC material for high flexural strength application. J. Eur. Ceram. Soc. **41**(2), 1342–1351 (2020)
2. T. Qin, C. Zhong, H. Yang et al., Investigation on glass-forming ability, Flexural strength and microwave dielectric properties of Al_2O_3-doped LMZBS glasses. Ceram. Int. **45**(8), 10899–10906 (2019)
3. K.F. Chan, M.H.M. Zaid, S. Liza et al., Tuning the Optical Bandgap of Multi-Walled Carbon Nanotube-Modified Zinc Silicate Glass-Ceramic Composites. Ceram. Int. **47**(14), 20108–20116 (2021)
4. F. Wang, Y.H. Lou, Z.J. Li et al., Improved flexural strength and dielectric loss in Al2O3-based LTCC with La_2O_3-CaO-B_2O_3-SiO_2 glass. Ceram. Int. **47**(7), 9955–9960 (2020)
5. F.Y. Huang, H. Su, Y.X. Li et al., Low-temperature sintering and microwave dielectric properties of CaMg1–xLi2xSi2O6 (x=0–0.3) ceramics. J. Adv.Ceram.9(4), 471-480 (2020)
6. H. Hsianga, C. C. Chen, S.Y. Yang., Microwave dielectric properties of $Ca_{0.7}Nd_{0.2}TiO_3$ ceramic-filled CaO-B_2O_3-SiO_2 glass for LTCC applications. J. Adv.Ceram. **8**(3), 345–351 (2019)
7. G. Dou, D.X. Zhou, M. Guo et al., Low-temperature sintered Mg_2SiO_4–$CaTiO_3$ ceramics with near-zero temperature coefficient of resonant frequency. J. Mater. Sci. Mater. in Electron. **24**, 1431–1438 (2013)
8. C. Zhang, R. Zuo, J. Zhang et al., Structure-dependent microwave dielectric properties and middle-temperature sintering of forsterite $(Mg_{1-x}Ni_x)_2SiO_4$ ceramics. J. Am. Ceram. Soc. **98**(3), 702–710 (2015)
9. Y.M. Lai, X.L. Tang, X. Huang et al., Phase composition, crystal structure and microwave dielectric properties of $Mg_{2-x}Cu_xSiO_4$ ceramics. J. Eur. Ceram. Soc. **38**, 1508–1516 (2018)
10. K.X. Song, X.M. Chen, C.W. Zheng, Microwave dielectric characteristics of ceramics in Mg_2SiO_4–Zn_2SiO_4 system. Ceram. Int. **34**(4), 917–920 (2008)
11. G. Dou, M. Guo, Y.X. Li et al., Effects of low melting point materials on sinterability and microwave dielectric properties of X_2SiO_4–$CaTiO_3$ (X=Mg, Zn) for LTCC. J. Mater. Sci. Mater. in Electron. **26**(11), 9195–9199 (2015)
12. J. Ma, T. Yang, Z. Fu et al., Low-fired Mg_2SiO_4-based dielectric ceramics with temperature stable for LTCC applications. J. Alloys. Compd. **695**(25), 3198-3201 (2016)
13. Y. Lai, C. Hong, L. Jin et al., Temperature stability and high-Qf of low temperature firing Mg_2SiO_4–Li_2TiO_3 microwave dielectric ceramics. Ceram. Int. **43**(18), 16167–16173 (2017)
14. T.S. Sasikala, M.N. Suma, P. Mohanan et al., Forsterite-based ceramic–glass composites for substrate applications in microwave and millimeter wave communications. J. Alloys. Compd. **461**(1–2), 555–559 (2008)
15. J. Zhang, Z.X. Yue, Y. Luo et al., Novel Low-Firing Forsterite-Based Microwave Dielectric for LTCC Applications. J. Am. Ceram. Soc. **99**(4), 1122–1124 (2016)
16. Z. Weng, R. Guan, Z. Xiong., Effects of the ZBS addition on the sintering behavior and microwave dielectric properties of $0.95Zn_2SiO_4$-$0.05CaTiO_3$ ceramics. J. Alloys. Compd. **695**(25), 3517-3521 (2016)
17. O.Y. Sang, H.S. Sang, K.S. Kim et al., Low-temperature preparation and microwave dielectric properties of ZBS glass–Al_2O_3 composites[J]. Ceram. Int. **35**(3), 1271–1275 (2009)
18. K.P. Surendran, P. Mohanan, M.T. Sebastian, The effect of glass additives on the microwave dielectric properties of $Ba(Mg_{1/3}Ta_{2/3})O_3$ ceramics. Journal of Solid State Chemistry **177**(11), 4031–4046 (2004)
19. Y.F. Liu, Y.H. Tan, S.G. Liu et al., Dielectric properties, microstructure and phase evolution of non-stoichiometric $0.9Mg_{2+x}SiO_{4+x}$-$0.1CaTiO_3$ microwave dielectric ceramics. Ceram. Int. **47**(23), 33798-33804 (2021)
20. X. Du, S. Hua, H. Zhang et al., Effects of Li-ion substitution on the microwave dielectric properties of low-temperature sintered ceramics with nominal composition $Li_{2x}Mg_{2-x}SiO_4$. Ceram. Int. **44**(2), 2300–2303 (2018)
21. Y.J. Eoh, H.J. Ahn, E.S. Kim., Effect of two-step sintering on the microwave dielectric properties of $Zn_{1.8}SiO_{3.8}$ ceramics. Ceram. Int. **41**, S544-S550 (2015)
22. R. Deshmukh, V. Chaware, R. Ratheesh et al., Synthesis and Microwave Dielectric Properties of BBSZ-Zinc Silicate Based Material for LTCC Applications. J. Mater. Sci. Mater. in Electron. **50**(3), 1323–1330 (2021)